

Developmental Independence of Median Fins From the larval Fin Fold Revises Their Evolutionary Origin

Kazuhide Miyamoto

Tohoku University

Koichi Kawakami

National Institute of Genetics

Koji Tamura

Tohoku University

Gembu Abe (✉ gembu.abe.b5@tohoku.ac.jp)

Tohoku University

Research Article

Keywords:

Posted Date: January 17th, 2022

DOI: <https://doi.org/10.21203/rs.3.rs-1223839/v1>

License: © ⓘ This work is licensed under a Creative Commons Attribution 4.0 International License.

[Read Full License](#)

Abstract

The median fins in modern fish that show separated forms (dorsal, anal, and caudal fins) are derived from a continuous fold-like structure, both in ontogeny and phylogeny. The median fin fold (MFF) hypothesis assumes that the median fins evolved by reducing some positions in the continuous fin fold of basal chordates, based on the classical morphological observation of developmental reduction in the larval fin folds of living fish. However, the developmental processes of median fins are still unclear at the cellular and molecular levels. Here, we describe the transition from the larval fin fold into the median fins in zebrafish at the cellular and molecular developmental level. We demonstrate that reduction does not play a role in the emergence of the dorsal fin primordium: the reduction occurs passively after the primordium formation, rather than actively scrapping the non-fin forming region by inducing cell death. We also report that the emergence of specific mesenchymal cells and their proliferation promote the dorsal fin primordium formation. Based on these results, we propose a revised hypothesis of median fin evolution in which acquisition of *de novo* developmental mechanisms is a crucial evolutionary component of the separated forms of median fins.

Introduction

Fish, defined as vertebrates without tetrapods in this article, are characterized by unique appendages called fins in their morph¹. Fish fins are classified into two groups: paired fins located at the ventral-lateral body trunk, and unpaired median fins situated on the body midline along the rostral-caudal axis^{1,2}. The median fins, which function by providing elaborate maneuvers in the water, show separated individual forms (dorsal, anal, and caudal fins)¹⁻⁵. These median appendages are of significant interest in evolutionary development, in that they are thought to have evolved from a continuous midline fold-like structure called the median fin fold (MFF) in basal chordates ('basal chordates' are defined as chordates other than the crown vertebrates in this article)⁶⁻⁸. In their development, fish median fins that are separated forms in adulthood are thought to be derived from a continuous fold-like structure in the embryonic or larval stage, called the larval median fin fold (LMFF)^{3,6,9-13}. That the evolutionary process may closely resemble the developmental process has been known for a long time.

For the evolutionary and developmental process of the median fins, an influential hypothesis, the MFF hypothesis, has been proposed^{1,2,6,8,12-16}. The MFF hypothesis assumes that the median fins evolved by reducing some positions in the MFF and retaining other parts^{6,8,12-16}. In this widely accepted hypothesis, the fin fold's reduction process is supposed to actively lead to the discontinuous individual median fins in fish. Indeed, we can see tissue reduction at inter-fin areas of the LMFF during development in some fish species (Fig. 1a-d)^{3,6,11,13,15,17-19}, and the median fin structures are raised at the remaining areas of the LMFF, supporting the hypothesis.

The median fins in teleosts are composed of proximal cartilaginous skeleton (pterygiophores) and distal dermal skeleton (fin rays)^{17,20-22}. As described above, these median fins develop through dynamic

morphological changes in the LMFF during their ontogeny^{3, 9-11,15, 17-19}, but their developmental processes are still poorly understood at the cellular and molecular levels. For instance, previous studies have supposed that the reduction of the LMFF is provided by apoptotic cell death^{15,23}, and cell death at the LMFF has been reported in some studies²³⁻²⁵. However, cell death at the LMFF has been examined only during the embryonic stage when the median fin primordia have not yet appeared. In addition, the fin mesenchymal cells immigrate into the LMFF from the somite-derivatives at two times, the early embryonic and the larval stage^{26,27}. Furthermore, the mesenchymal cells that give rise to the median fin skeleton have been reported to come from the later stage at around two weeks post-fertilization²⁷. It is still possible that additional developmental mechanisms other than reduction may contribute to median fin formation in post-embryonic development. The MFF hypothesis should be further examined and revisited from a developmental biological viewpoint.

In this work, we examined the transition from the LMFF into the dorsal fin in zebrafish at the levels of cellular and molecular developmental biology. We describe median fin morphogenesis in post-embryonic zebrafish larvae, and we also detected cell death and observed epithelial cell mass behavior in the reducing LMFF areas. Furthermore, we observed mesenchymal cell behavior, including their distribution, differentiation, and proliferation, and assessed the role of FGF signaling in dorsal fin primordia. Based on our results, we propose a revised hypothesis of median fin evolution from both developmental and phylogenetic views.

Results

The timing of dorsal fin development is different from LMFF reduction.

We first examined the initiation process of dorsal fin formation in the LMFF (Fig. 1). In 4.2 mm standard length (SL) zebrafish, the continuous LMFF looks to have no protrusions or outgrowth that imply a fin primordial structure at the dorsal, caudal, and ventral midline (Fig. 1a, a'). When the larval size reaches 5.6 mm SL, a small dorsal area in the LMFF began outgrowth (white arrowhead in Fig. 1b'). In 6.3 mm SL zebrafish, the outgrowth site continues to grow distally and expand along the rostral-caudal axis (white arrowhead in Fig. 1c'). By 7.2 mm SL, the dorsal fin primordium with fin rays is visible. In 7.2 mm SL zebrafish, the height of the LMFF looks reduced from the anterior side both before and behind the dorsal fin; thus, the dorsal and caudal fins separated to form independent structures (Fig. 1d, d'). Taken together, we estimated that the dorsal fin outgrowth at 5.6 mm SL may be the initial dorsal fin primordium.

To examine the detailed process of dorsal fin formation and LMFF reduction, we quantitatively analyzed the height of the LMFF every five days in the transition process from 5 days post-fertilization (dpf) to 20 dpf (n=6, Fig. 1e-h). We measured the height of the LMFF at the future dorsal fin-appearing position (red lines in Fig. 1e, f) and at the LMFF-disappearing position behind the dorsal fin (blue lines in Fig. 1e, f). The height of the LMFF at the dorsal fin position increased moderately as a protrusion between 4.5-5.0 mm SL and then started to increase rapidly for outgrowth at around 5.0 mm SL (red dots and lines in Fig. 1g, h). The rapid increase continued until 7.0 mm SL. In contrast, the height of the LMFF at the

presumptive disappearing position behind the dorsal fin was almost constant between 4.0–5.5 mm SL (blue dots and lines in Fig. 1g, h). Then, the height of that region started decreasing at around 5.5 mm SL and later decreased rapidly until 7.0 mm SL.

These data suggest that the LMFF protrusion and outgrowth at the future site of the dorsal fin precedes the reduction of the LMFF. In other words, the emergence of the dorsal fin may not be due to the process of LMFF reduction, but rather depends on its protrusion.

Signals for apoptotic cell death could not be detected in the reduction process of the LMFF.

Since dorsal fin appearance precedes the LMFF reduction, this raises the question of whether cell death in the LMFF provokes dorsal fin formation. We therefore investigated cell death in the process of the LMFF reduction. First, we performed acridine orange staining, which identifies cell death in living specimens^{28,29}, at the LMFF-reducing stage (6.0–6.5 mm SL, n = 6; 6.5–7.0 mm SL, n = 6; 7.0–7.5 mm SL, n = 5) (Fig. 2a–c’). We found no obvious signal for cell death in the reducing LMFF area in any samples (Fig. 2a, a’, b, b’, c, c’). We detected some signals in different areas such as at the base of the caudal fin, indicating that our experimental procedure for the staining was fine. We further performed whole-mount immunohistochemistry with an anti-active caspase antibody at the LMFF-reducing stage (6.0–6.5 mm SL, n=6; 6.5–7.0 mm SL, n=5; 7.0–7.5 mm SL, n=5) (Fig. 2d–f’)³⁰. We detected some positive cells at the base of the caudal fin (Fig. 2d”, e”, f”), indicating that the immunohistochemistry detected dying cells correctly. We found very few positive signals in the reducing LMFF area (Fig. 2d’, e’, f’) in all samples.

These data show that cell death did not occur in the reducing LMFF area. In conclusion, cell death may not play a role in LMFF reduction and median fin segregation.

Cell shape change and cell migration in LMFF reduction.

Our above results suggest that cellular behaviors other than cell death may play a role in the process of the LMFF reduction. We focused on epithelial cell migration and cell shape change in LMFF reduction and performed *in vivo* cell-tracking analysis with an epidermal cell-specific *cre*-expressing vector (*krt8-p:cre*)³¹. We injected the *krt8-p:cre* vector into *Tg(actbp-loxP-DsRed-loxP-EGFP)*³² embryos (Fig. 3a) and observed EGFP-positive epidermal cells that were distributed as mosaic patches in the LMFF of the injected specimens (Fig. 3c–f’). We traced the epidermal cell behavior from the stages when the LMFF reduction started (12 dpf, 5.8–6.1 mm SL, n = 3), and specimens were observed every two days until 16 dpf, when their size was around 7.0 mm SL (Fig. 3b). Figure 3 shows a specimen in which two GFP-positive populations of epidermal cells can be detected in the reducing LMFF (yellow dotted area in Fig. 3c). During the observation period, GFP-positive populations became narrow along the proximal-distal axis by shape change, in which each cell began proximo-distal shrinkage (magenta bracket in Fig. 3d’, e’, f’) and migrated down to the trunk (magenta arrowheads in Fig. 3d’, e’, f’).

These results indicate that epidermal cells collectively deform proximo-distally and migrate from the LMFF to the body trunk, suggesting that deformation and migration of LMFF epidermal cells contributes to the process of LMFF reduction.

Mesenchyme growth in the dorsal fin primordium Our morphological observations (Fig. 1) also suggest that the protrusion and outgrowth of the LMFF is a key process in dorsal fin formation, rather than the LMFF reduction process. Previous studies have shown that somite-derived mesenchymal cells are condensed in the future site of the dorsal fin, and these mesenchymal cells develop into dorsal fin skeletal elements^{18,27}. These studies, however, have not shown when mesenchymal cells emerge or the differentiation process of the mesenchyme. Thus, we investigated mesenchymal cell behavior during the formation of the dorsal fin primordium by analyzing a reporter transgenic fish line.

We observed reporter expression in the *gt1116A* transgenic line (Fig. 4). In *gt1116A*, the gene-trapping *gal4* construct was integrated within the *prdm16* gene, and the UAS:EGFP reporter was found to be expressed in mesenchymal cell populations of the early pectoral fin bud^{33,34}. In addition, UAS:EGFP in *gt1116A* has been reported to be expressed in other developing median fins, including the dorsal fin³⁴. We first examined whether EGFP expression patterns of *gt1116A* are valid as a reporter of the fin mesenchyme in the developing dorsal fin primordium. The reporter EGFP was detected in median fin formation at the stage when the LMFF of the future dorsal fin site starts protruding (Fig. 4a; SL = 5.0–5.5 mm). Transverse sections showed UAS:EGFP expression distributed in cells of the middle at the LMFF protrusion, sandwiched by two outer layers of cells (presumably epidermal layers) where no signal was detected (Fig. 4b–b’). These data confirmed that UAS:EGFP in the *gt1116A* line is expressed in the mesenchymal cells of the dorsal fin primordium.

We next assessed the expression pattern of the UAS:EGFP reporter in the *gt1116A* line in the transition from LMFF to dorsal fin primordium while observing chondrocytes by *sox10:DsRed* (4.0–4.5 mm SL, n = 6; 6.5–7.0 mm SL, n = 5; 7.0–7.5 mm SL, n = 5) (Fig. 4c–f’). In 4.0–4.5 mm SL zebrafish, which are before the protrusion of the LMFF (Fig. 1h), no EGFP-positive cells were observed in the future site of the dorsal fin (white bracket in Fig. 4d). In 4.5–5.0 mm SL zebrafish, when the LMFF begins protruding (Fig. 1h), a mass of EGFP-positive cells was observed in the future site of the dorsal fin (white bracket in Fig. 4e). In 5.0–5.5 mm SL zebrafish with the LMFF outgrowth, the EGFP-positive mesenchymal cell population expanded distally (white bracket in Fig. 4f). The DsRed-positive cartilaginous elements, which become pterygiophores (basal elements of the dorsal fin skeleton), emerged at the lower part of the mesenchymal cell population (Fig. 4f’). In addition, because the site of the cartilage formation matched the distal expansion of the EGFP-positive mesenchymal cell population, these cells may give rise to the fin rays (white arrowheads in Fig. 4f’). These data suggest that EGFP-positive cells of the *gt1116A* line develop dorsal fin skeletal elements, such as pterygiophores and fin rays. Thus, the dorsal fin-specific developmental mechanisms with mesenchymal cells, at least as defined by expression of *prdm16A*, appeared simultaneously with the protrusion of the LMFF at 4.5–5.0 mm SL, and we define the protrusion with *prdm16A*-positive mesenchyme as the initial dorsal fin primordium.

Cell proliferation in dorsal fin mesenchyme

An analysis of the *gt1116A* line suggested that the development of the dorsal fin primordial mesenchyme is associated with the protrusion of the LMFF, which raises the question of whether cell proliferation in the fin mesenchyme may contribute to dorsal fin primordium development. To identify the distribution of proliferating cells in the dorsal fin primordium, we performed wholemount immunohistochemistry with an anti-phospho histone H3 (pH3) antibody^{30,34}. In 4.5–5.0 mm SL zebrafish (n=6) (Fig. 5a, b), a few pH3-positive cells were detected within the dorsal fin primordium in some samples (n=2/6). In many samples (n=10/12) of 5.0–5.5 mm SL zebrafish, pH3-positive cells were detected, though the number of positive cells was still few (Fig. 5c, d). In 5.5–6.0 mm SL zebrafish, all samples (n=7/7) showed many pH3-positive cells in the dorsal fin primordium (Fig. 5e, f). Fig. 5g (optical sections of the dorsal fin primordium) shows that pH3-positive cells were located in the middle of the dorsal fin primordium, indicating that these are mesenchymal (Fig. 5g). Quantitative analysis confirmed that the number of pH3-positive cells in the dorsal fin primordium increases along with body growth from 4.5 to 6.0 mm SL (Fig. 5h). Interestingly, the stage when the proliferation of the mesenchymal cells starts increasing corresponds with the stage when the height of the dorsal fin primordium starts increasing rapidly for outgrowth (5.0 mm SL, Fig. 1h). This suggests that mesenchymal cell proliferation plays a role in the outgrowth of the dorsal fin primordium.

In some fish such as sharks and cichlids, it has been shown that FGF signaling works in dorsal fin development^{19,35}. In larval zebrafish, it has also been shown that FGF signaling play roles in early processes of LMFF development¹⁰. Therefore, we sought to investigate the role of FGF signaling in the cell proliferation of the dorsal fin primordium. SU5402 is a chemical inhibitor of Fgfr that has been reported to specifically inhibit the kinase activity of nearly all types of Fgfr^{10,36,37}. Treatment for three days with SU5402 at 5.0–5.5 mm SL resulted in no significant effect on cell proliferation in the early dorsal fin primordium (Fig. 5i, S1a). These results suggest that FGF signaling may not play a role in the early proliferation of dorsal fin mesenchymal cells (5.0–6.0 mm SL). In anal fins, on the other hand, SU5402 treatments at 5.0–5.5 mm SL inhibited cell proliferation (Fig. S1b). It is possible that FGF signaling may play a role in the later stages of median fin development, since anal fin development greatly precedes dorsal fin development. Furthermore, SU5402 treatment also did not affect the height of the dorsal fin primordium when zebrafish were between 5.0 and 6.0 mm SL (Fig. S1c, d). Taken together, these data suggest that FGF signaling does not play a role in at least the initial protrusion process of dorsal fin primordium.

Discussion

The developmental process critical for median fin formation.

The separated median fins in modern fish evolved from the continuous MFF in the basal chordate, resembling the developmental process derived from the LMFF^{6,8,12,13,15}. Based on this resemblance, the

MFF hypothesis argues that reduction of the fin fold is a key evolutionary process of the segregation among independent median fins in vertebrate phylogeny from the view of recapitulation theory^{6,8,14–16,15}. This is because of the classical assumption that fish median fin development is caused by the simple reduction process of the LMFF. However, our present study revealed that the reduction of the LMFF occurred after the LMFF protrusion in the future site of dorsal fin formation (Fig. 1). Furthermore, although previous studies supposed that LMFF reduction is caused by apoptosis along the inter-fin areas of the LMFF^{15,23,25}, our data suggest that cell death did not play a role in LMFF reduction (Fig. 2). So, how does the reduction of the LMFF occur during the zebrafish ontogeny? Our cell-tracking analyses revealed cell behaviors such as narrowing proximo-distally and migrating to the body trunk region (Fig. 3). During the developmental period when LMFF reduction occurs, zebrafish larvae vigorously increase in body size (both length and width). So LMFF epithelial tissue may be involved in this body surface expansion, stretching along the anterior-posterior axis and moving to the trunk region. It is noteworthy that this collective migration of epidermal cells is seen at relatively later stages when the dorsal fin primordium has already protruded and the LMFF has reduced. This suggests that LMFF reductions are passive and do not drive the emergence of median fin primordia. We postulate that regression or degradation of the supporting material in the LMFF structure, such as actinotrichia and laminin^{38–41}, caused the epithelial migration in the trunk at the inter-fin area. Further molecular developmental biological studies are required to reveal how this collective epithelial cell movement occurs. Together with our cell behavioral analyses, we suggest that the reduction of the LMFF does not cause dorsal fin formation. Instead, the LMFF reduction is a passive reaction during body size increase. In other words, other cellular and developmental dynamics could be responsible for dorsal fin formation during ontogeny.

What kinds of cellular developmental mechanisms play a role in dorsal fin formation? From examining the appearance of the dorsal fin primordium, our data show that the dorsal fin primordial mesenchyme, which expresses UAS:EGFP in the *gt1116A* line and develops into the adult fin skeleton (Fig. 4), emerges simultaneously with the LMFF protrusion (Fig. 1). Due to *gt1116A* trapping *prdm16*, we suggest that developmental mechanisms that specify the mesenchymal cell population expressing developmental genes, such as *prdm16*, play a role in dorsal fin primordium formation. The rapid increase in the LMFF height in the dorsal fin primordium at around 5.0 mm SL correlates to the appearance of proliferation of mesenchymal cells (Fig. 5c-h), suggesting that this cell proliferation promotes the outgrowth of the dorsal fin primordium. In addition, cell migration may also contribute to dorsal fin development along with cell proliferation. In 4.5–5.0 mm SL zebrafish in our data, most samples did not have cell proliferation signals as detected by anti-pH3 antibody in the dorsal fin primordium. In 5.0–5.5 mm SL zebrafish in our data, the number of pH3-positive cells was relatively small compared to the total number of dorsal fin primordial mesenchymal cells (Fig. 5h). Previous studies have shown that fin osteoblasts are derived from a secondary source of somite-derived cells, not from cells present in the LMFF before the hatching period^{26,27}. We suggest that migration of the somite-derivative cells into the fin primordium at the initiation of the protrusion stage in particular and the later outgrowth stage contributes to the increase of mesenchymal cell mass in the dorsal fin primordium. In addition, although FGF signaling contributes to initial LMFF formation¹⁰, our pharmacological assays showed that this mechanism does not play a role

in the early outgrowth phases of dorsal fin primordia (Fig. 5i and Fig. S1b, c). This discrepancy in molecular signaling mechanisms between early induction of the LMFF and later outgrowth at the dorsal fin primordium suggest that the developmental modules associated with the dorsal fin primordium are independent of those involved in LMFF formation. Previous studies have shown that some zebrafish mutants with malformed LMFFs, which are bubbly or collapsed edge of the fin fold, develop normal adult median fins⁴². This evidence supports our inference that the developmental module of the dorsal fins behaves independently from the LMFF developmental module.

Revision of the evolutionary event essential for acquiring median fins.

Our ontogenetical evidence does not agree with the MFF hypothesis. Thus, we would revise the phylogenetic assumptions concerning the critical developmental mechanisms that are responsible for evolving the separated form of median fins.

The MFF hypothesis predicts that separated median fins appeared by acquiring a mechanism to transition from the LMFF to median fins, based on the premise that the fish LMFF is homologous to the plesiomorphic MFF of basal chordates. The lower Cambrian basal chordates *Haikouichthys* and *Mylokommingia* had many anatomical structures that inform the taxonomic affinity of stem vertebrates⁴³⁻⁴⁵. They had an MFF, though previous studies lacked enough evidence to confirm the presence of endoskeletal elements⁴⁴⁻⁴⁶. Thus, it was naturally assumed that animals in the lineage from basal chordates to early vertebrates continuously possessed MFFs, and that fish LMFFs are homologous to these MFFs^{15,46,47}. Addition to this premise, the MFF hypothesis presumes that median fin development occurred by a reduction of the inter-fin region based on morphological observations of ontogeny in living fish^{2,6,8,12-14}. From this phylogenetic and ontogenetic representation, the MFF hypothesis implies that the median fins evolved from ancestral MFFs by acquiring reduction mechanisms (REFs). However, our study of the ontogenetic process from LMFFs to median fins suggests that median fin-associated developmental modules behave independently from the LMFF developmental module. We hypothesize that acquiring the developmental process of LMFF reduction is not the main contributor to the evolution of median appendages. Rather, acquiring *de novo* developmental processes in which a mesenchymal cell mass invades into the LMFF and expresses a specific genetic program for developing adult median fins is the key evolutionary component of the separated form of median fins. Further investigations of the developmental processes in various fish, such as cyclostomes and chondrichthyans, will help test our hypothesis of the phylogenetic process of acquiring median fins and will further illuminate the origin of fin skeletal components such as fin rays and pterygiophores.

Differences between median fins and paired fins in development

The evolutionary origin of paired fins is also thought to be related to median fin evolution. Paired fins in most fish exhibit the basic skeletal configuration seen in median fins, with a basal endoskeleton and

associated fin rays^{2,4}. One influential idea assumes that paired fins arose by co-option of the genetic patterning modules established during median fin evolution^{17,48,49}. Indeed, gene expression studies in paired and median fins have identified a similar pattern in the expression of developmental genes, such as the nested expression of Hox genes^{19,35,48-50}. We found that *prdm16* is expressed in dorsal fin mesenchyme by observations of EGFP expressions in the *gt1116A* line, and this gene is also expressed in pectoral fin mesenchyme at the early embryonic stage^{34,51,52}. Our and previous studies indicate that *prdm16*-positive mesenchymal cells differentiate into skeletal elements in both pectoral and dorsal fins³⁴. This gene expression pattern suggests that median and paired fins share the developmental mechanisms and supports the hypothesis that the developmental mechanism of mesenchymal cells was co-opted from median fins to paired fins. However, although FGF signaling plays an essential role in pectoral fin buds at the early embryonic stage^{53,54}, our pharmacological assays with an FGF signaling inhibitor showed no apparent effect on the early development of dorsal fins (Fig. 5i, S1). Based on these similarities and differences, our hypothesis of paired fin origins holds that paired fins arose by partial co-option of ancestral genetic modules that were first present in median fins.

Methods

Zebrafish strains.

The following transgenic zebrafish lines were used in this study: *gt1116A* (*gSAIzGFFD1116A:Gal4FF;UAS:EGFP*, trapping the *prdm16* gene)³⁴ and *sox10:DsRed*^{55,56}. To generate *krt8-p:Cre* (*keratin8 enhancer:gata2 promoter:Cre*) transgenic fish, we injected the *krt8-p:Cre* plasmid with *Tol2* transposase mRNA into *actb-p:loxP-RFP-loxP-GFP* eggs³². To prepare *krt8-p:Cre*, genomic DNA fragments were isolated by using PCR (Fwd: GAG TCG ACG CCT TTG AAA TGT AAA AGC TCA, Rev: ATC CTG CCT TGT GTG TTT TCT GTC TTG T)³¹ and integrated with a downstream *Cre* gene into the *tol2* plasmid⁵⁷.

Zebrafish were housed at 28°C under light for 14 h⁵⁸, and the standard length (SL) of individuals was measured¹⁸. To indicate the body sizes of individuals, we used SL instead of the date of development, since zebrafish of the same age often have different body sizes¹⁸. All experimental animal care was in accordance with institutional and national guidelines and regulations and was approved by the Tohoku University Animal Research Committee (Permit Number: 2019LsA-022). The study was carried out in compliance with the ARRIVE guidelines.

Observation of zebrafish Tg.

Zebrafish larvae less than 6.0 mm SL were anesthetized with 0.025% MS222/E3 and then embedded in 2% methylcellulose/E3 on a slide-glass, dropping 0.125% MS222/E3. Specimens more than 6.0 mm SL were anesthetized with 0.025% MS222/E3 and located on a 1% agarose-gel/E3. These zebrafish were observed by a microscope (Leica M205 FA) and photographed with a camera (Leica DFC 360 FX).

Images were obtained and analyzed with Leica LAS-AF, LAS-X, and Adobe Photoshop CS6 after observation, and then the larvae were immediately transferred to a small case filled with system water and awakened by sprayed water.

LMFF/dorsal fin primordium height measurements.

LMFF/dorsal fin primordia heights were measured as described below. LMFF/dorsal fin primordia were observed by a microscope (Leica M205 FA) and photographed with a camera (Leica DFC360 FX). To reduce variance in the measured length from the photographs, the photograph capture and arrangement were repeated three times. LAS AF Lite was used to measure the standard length, fin primordium, and LMFF from the photographs. The mean of three measurements was used in the analysis.

To examine the height of the LMFF/dorsal fin primordium at the same position during ontogeny, we used the somite boundary, which is located at the gut tube bending point (purple arrowhead in Fig. 1e, f) as a landmark (the first boundary, purple line in Fig. 1e, f). Then, we measured two somite boundaries: the next somite boundary (red line in Fig. 1e, f) and the fourth somite boundary from the first boundary (Fig. e, f, blue lines). In larvae less than about 6.0 mm SL, which have “V”-shaped somites, we measured the height of the LMFF/dorsal fin primordium from the cross point of the somite boundary and the border of the trunk to the distal tip of the dorsal fin primordium/LMFF (red and blue lines in Fig. 1e). In larvae more than about 6.0 mm SL, which have “W”-shaped somites, we measured the height of the LMFF/dorsal fin primordium from the cross point (Fig. 1f) of the extension line of the middle part of this somite boundary (dashed red and blue line in Fig. 1f) and border of the trunk to the distal tip of the dorsal fin primordium/LMFF (red and blue lines in LMFF in Fig. 1f).

Immunohistochemistry.

Whole mount immunohistochemistry for detecting cell death (anti-Caspase-3, #ab13847, Abcam) and mitosis (Mouse monoclonal anti-pH3, #9706, Cell Signaling Technology) was performed as previously described^{30,34} with minor modifications. Zebrafish larvae of the suitable stage were collected during observation with a microscope (Leica M165C), fixed with 4% PFA/PBS, and dehydrated with methanol/PBT (0.1% Tween-20 in PBS). Samples were blocked with 2% BSA, 1% goat serum, and 1% DMSO in PBT. The head and abdomen were eliminated from the samples to prepare them for observation. The samples were placed on a glass slide, covered with a coverslip, lightly pressed, and observed with a confocal microscope (Leica TCS SP5 II).

Section immunofluorescence staining was performed as previously described⁵⁹ with minor modifications. Frozen sections of fixed zebrafish were prepared with a cryostat (Leica CM3050 S). The sections were washed in PBT three times for 5 min. After 1 h of blocking with 1% blocking reagent (#11096176001, Roche) in PBT, the sections were incubated overnight at 4°C with a 1:1000 dilution of anti-GFP antibody (anti-green fluorescent protein, #A11120, Invitrogen). They were washed three times in PBT and incubated with a 1:500 dilution of secondary antibody (anti-mouse Alexa Flour 488 goat anti-mouse IgG, #A11001, Invitrogen) and a 1:25,000 dilution of DAPI for 30 min. After washing four times in

PBT, samples were sealed by VECTASHIELD (#H-1000, Vector Laboratories). The samples were then observed with a confocal microscope (Leica TCS SP5 II).

Acridine orange staining.

Acridine orange (AO; #A6014-10G, Sigma) was used to identify cell death including apoptosis^{28,29} following the method of Freitas et al.²⁷. Embryos were incubated in 0.5 µg/ml AO in PBS at room temperature for 30 min in the dark and rinsed in fish water for 10 min three times. Samples were observed by a microscope (Leica M205 FA) and photographed with a camera (Leica DFC 360 FX) under UV fluorescence.

SU5402 treatment.

Inhibition of signaling through FGF receptors was performed with the lipophilic reagent SU5402 (#572630, CalBiochem)³⁷. Embryos were incubated in the dark at 28.5°C with 20 µM SU5402 in fish water, prepared from 5 mM SU5402 stock solution in DMSO^{10,60}. Control embryos were incubated with the corresponding amount of DMSO. After treatment, some samples were fixed in 4% PFA in PBS for 16–24 h, and cell mitosis was detected by immunohistochemistry. In the other samples, the height of the fin primordium was examined by a microscope (Leica M205 FA) and photographed with a camera (Leica DFC 360 FX).

Statistical analysis.

Scatter plots, which show the transition of the height of the LMFF/dorsal fin primordium, and box plots, which show the number of proliferating cells in the median fin primordium, were generated with the R (<https://www.r-project.org/>) package ggplot2. The local polynomial regression fit shown in Fig. 1h, which is the transition of the height of the LMFF/dorsal fin primordium, was obtained using the loess method. The local polynomial regression lines and R squared values were computed in R (ggplot, method=lm). For quantitative analysis of the number of proliferating cells in median fin primordium, Welch's *t* test was performed in R using the t.test function. For quantitative analysis of the pharmacological effects on the height of LMFF/dorsal fin primordium, analysis of covariance (ANCOVA) between groups was computed in R using the ANOVA function.

Declarations

Data availability

The datasets used and/or analysed during the present study are available from the corresponding author on reasonable request.

Acknowledgments

We thank Dr. Tohru Yano (The Jikei University School of Medicine, Japan) for the kind gift of the zebrafish *krt8* promoter plasmid. We also thank the members of Tamura's laboratory for critical comments on this study and manuscript. This work was supported by JSPS KAKENHI Grant Numbers JP21K19202, JP21H05768, JP20H05024, and JP18H02446 to K.T.; JSPS KAKENHI Grant Numbers JP16K18546, JP18K06239, and JP20H04854 to G.A; JSPS KAKENHI Grant Number JP21H02463 to K.K.; NBRP from MEXT JP21km0210087 to K.K.; and the Sasakawa Scientific Research Grant to K.M.

Author contributions statement

K.M., G.A., and K.T. designed the experiments. K.M. performed the experiments. K.K. and G.A. developed the transgenic fish lines used in this work. K.M., T.K., and G.A. interpreted the data and prepared the initial draft of the manuscript. All authors commented on and modified the draft. All authors read and approved the final manuscript.

Competing Interests

The authors declare no competing interests.

References

1. Larouche, O., Zelditch, M. L. & Cloutier, R. A critical appraisal of appendage disparity and homology in fishes. *Fish Fish.* **20**, 1138–1175 (2019).
2. Romer, A. S. & Parsons, T. S. *The vertebrate body*. (Saunders College, 1986).
3. Bemis, W. E. & Grande, L. Development of the median fins of the North American paddlefish (*Polyodon spathula*), and a reevaluation of the lateral fin-fold hypothesis. *Mesozoic Fishes 2 - Syst. Foss. Rec.* **2**, 41–68 (1999).
4. Kardong, K. V. *Vertebrates: comparative anatomy, function, evolution*. (McGraw-Hill Education, 2019).
5. Helfman, G. S., Collette, B. B., Facey, D. E. & Bowen, B. W. *The diversity of fishes: biology, evolution, and ecology*. (Wiley-Blackwell, 2009).
6. Goodrich, E. S. (Edwin S. Studies on the structure & development of vertebrates. 837 (1930).
7. Nishino, A. & Satoh, N. The simple tail of chordates: Phylogenetic significance of Appendicularians. *Genesis* **29**, 36–45 (2001).
8. Thacher, J. Median and paired fins, a contribution to the history of vertebrate limbs. *Trans. Connect. Acad.* **3**, 281–310 (1877).
9. Dane, P. J. & Tucker, J. B. Modulation of epidermal cell shaping and extracellular matrix during caudal fin morphogenesis in the zebra fish *Brachydanio rerio*. *J. Embryol. Exp. Morphol.* **87**, 145–161 (1985).
10. Abe, G., Ide, H. & Tamura, K. Function of FGF signaling in the developmental process of the median fin fold in zebrafish. *Dev. Biol.* (2007) doi:10.1016/j.ydbio.2006.12.040.

11. Suzuki, T. *et al.* Differentiation of chondrocytes and scleroblasts during dorsal fin skeletogenesis in flounder larvae. *Dev. Growth Differ.* **45**, 435–448 (2003).
12. F.M. Balfour. On the development of the skeleton of paired fishes of Elasmobranchii. *Proc. Zool. Soc. London*, **iv**, 662–671 (1881).
13. F.M. Balfour. *A monograph on the development of elasmobranch fishes.* (Macmillan, 1878).
14. Cole, N. J. & Currie, P. D. Insights from sharks: Evolutionary and developmental models of fin development. *Dev. Dyn.* **236**, 2421–2431 (2007).
15. Stewart, T. A., Bonilla, M. M., Ho, R. K. & Hale, M. E. Adipose fin development and its relation to the evolutionary origins of median fins. *Sci. Rep.* **9**, 1–12 (2019).
16. Mivart, S. G. *Notes on the fins of Elasmobranchs, with considerations on the Nature and Homologues of Vertebrate Limbs.* (Longmans, Green, Reader, and Dyer, 1879).
17. Mabee, P. M., Crotwell, P. L., Bird, N. C. & Burke, A. N. N. C. Evolution of Median Fin Modules in the Axial Skeleton of Fishes. **90**, 77–90 (2002).
18. Parichy, D. M., Elizondo, M. R., Mills, M. G., Gordon, T. N. & Engeszer, R. E. Normal Table of Postembryonic Zebrafish Development: Staging by Externally Visible Anatomy of the Living Fish. 2975–3015 (2009) doi:10.1002/dvdy.22113.
19. Freitas, R., Zhang, G. J. & Cohn, M. J. Evidence that mechanisms of fin development evolved in the midline of early vertebrates. *Nature* **442**, 1033–1037 (2006).
20. Eaton, T. H. Skeletal supports of the median fins of fishes. *J. Morphol.* **76**, 193–212 (1945).
21. Lindsey, C. C. Evolution of meristic relations in the dorsal and anal fins of teleost fishes. *Trans. Roy. Soc. Canada Sect. 5* **49** 35-49 (1955).
22. Bird, N. C. & Mabee, P. M. Developmental Morphology of the Axial Skeleton of the Zebrafish, *Danio rerio* (Ostariophysi: Cyprinidae). *Dev. Dyn.* **228**, 337–357 (2003).
23. Cole, L. K. & Ross, L. S. Apoptosis in the developing zebrafish embryo. *Dev. Biol.* **240**, 123–142 (2001).
24. Nathaniel Abraham. Role of Programmed Cell Death in Defining Zebrafish Development. (2004).
25. Zuzarte-Luís, V. and Hurlé, J. Apoptosis in Fin and Limb Development. in *Fins into Limbs: Evolution, Development, and Transformation.* 103–108. (University of Chicago Press, 2008). doi:https://doi.org/10.7208/9780226313405-009.
26. Lee, R. T. H., Knapik, E. W., Thiery, J. P. & Carney, T. J. An exclusively mesodermal origin of fin mesenchyme demonstrates that zebrafish trunk neural crest does not generate ectomesenchyme. *Dev.* **140**, 2923–2932 (2013).
27. Ho Lee, R. T., Thiery, J. P. & Carney, T. J. Dermal fin rays and scales derive from mesoderm, not neural crest. *Curr. Biol.* **23**, R336–R337 (2013).
28. Hammerschmidt, M. *et al.* *dino* and *mercedes*, two genes regulating dorsal development in the zebrafish embryo. 95–102 (1996).

29. Freitas, R., Zhang, G. J. & Cohn, M. J. Biphasic Hoxd gene expression in shark paired fins reveals an ancient origin of the distal limb domain. *PLoS One* **2**, (2007).
30. Sousa, S. *et al.* Differentiated skeletal cells contribute to blastema formation during zebrafish fin regeneration. *Development* **138**, 3897–3905 (2011).
31. Gong, Z. *et al.* Green fluorescent protein expression in germ-line transmitted transgenic zebrafish under a stratified epithelial promoter from Keratin8. *Dev. Dyn.* **223**, 204–215 (2002).
32. Yoshinari, N., Ando, K., Kudo, A., Kinoshita, M. & Kawakami, A. Colored medaka and zebrafish: Transgenics with ubiquitous and strong transgene expression driven by the medaka β -actin promoter. *Dev. Growth Differ.* **54**, 818–828 (2012).
33. Asakawa, K. *et al.* Genetic dissection of neural circuits by Tol2 transposon-mediated Gal4 gene and enhancer trapping in zebrafish. *Proc. Natl. Acad. Sci. U. S. A.* **105**, 1255–1260 (2008).
34. Yoshida, K., Kawakami, K., Abe, G. & Tamura, K. Zebrafish can regenerate endoskeleton in larval pectoral fin but the regenerative ability declines. *Dev. Biol.* **463**, 110–123 (2020).
35. Höch, R., Schneider, R. F., Kickuth, A., Meyer, A. & Woltering, J. M. Spiny and soft-rayed fin domains in acanthomorph fish are established through a BMP-gremlin-shh signaling network. *Proc. Natl. Acad. Sci. U. S. A.* **118**, 1–8 (2021).
36. Fürthauer, M., Reifers, F., Brand, M., Thisse, B. & Thisse, C. Sprouty4 acts in vivo as a feedback-induced antagonist of FGF signaling in zebrafish. *Development* **128**, 2175–2186 (2001).
37. Mohammadi, M. *et al.* Structures of the tyrosine kinase domain of fibroblast growth factor receptor in complex with inhibitors. *Science (80-)*. **276**, 955–960 (1997).
38. Carney, T. J. *et al.* Genetic analysis of fin development in zebrafish identifies furin and Hemicentin1 as potential novel fraser syndrome disease genes. *PLoS Genet.* **6**, (2010).
39. Kuroda, J., Itabashi, T., Iwane, A. H., Aramaki, T. & Kondo, S. The Physical Role of Mesenchymal Cells Driven by the Actin Cytoskeleton Is Essential for the Orientation of Collagen Fibrils in Zebrafish Fins. *Front. Cell Dev. Biol.* **8**, 1–16 (2020).
40. Kuroda, J., Iwane, A. H. & Kondo, S. Roles of basal keratinocytes in actinotrichia formation. *Mech. Dev.* **153**, 54–63 (2018).
41. Webb, A. E. *et al.* Laminin α 5 is essential for the formation of the zebrafish fins. *Dev. Biol.* **311**, 369–382 (2007).
42. Van Eeden, F. J. M. *et al.* Genetic analysis of fin formation in the zebrafish, *Danio rerio*. *Development* **123**, 255–262 (1996).
43. Miyashita, T. *et al.* Hagfish from the Cretaceous Tethys Sea and a reconciliation of the morphological-molecular conflict in early vertebrate phylogeny. *Proc. Natl. Acad. Sci. U. S. A.* **116**, 2146–2151 (2019).
44. Shu, D. G. *et al.* Head and backbone of the Early Cambrian vertebrate Haikouichthys. *Nature* **421**, 526–529 (2003).
45. Shu, D. G. *et al.* Lower Cambrian vertebrates from south China. *Nature* **402**, 42–46 (1999).

46. Zhang, X. G. & Hou, X. G. Evidence for a single median fin-fold and tail in the Lower Cambrian vertebrate, *Haikouichthys ercaicunensis*. *J. Evol. Biol.* **17**, 1162–1166 (2004).
47. Bobb Schaeffer. Deuterostome Monophyly and Phylogeny. *Evol. Biol.* **21**, 179–235 (1987).
48. Letelier, J. *et al.* A conserved Shh cis-regulatory module highlights a common developmental origin of unpaired and paired fins. *Nat. Genet.* **50**, 504–509 (2018).
49. Freitas, R., Gómez-Skarmeta, J. L. & Rodrigues, P. N. New frontiers in the evolution of fin development. *J. Exp. Zool. Part B Mol. Dev. Evol.* **322**, 540–552 (2014).
50. Dahn, R. D., Davis, M. C., Pappano, W. N. & Shubin, N. H. Sonic hedgehog function in chondrichthyan fins and the evolution of appendage patterning. *Nature* **445**, 311–314 (2007).
51. Ando, H. *et al.* Lhx2 mediates the activity of Six3 in zebrafish forebrain growth. *Dev. Biol.* **287**, 456–468 (2005).
52. Ding, H. L., Clouthier, D. E. & Artinger, K. B. Redundant roles of PRDM family members in zebrafish craniofacial development. *Dev. Dyn.* **242**, 67–79 (2013).
53. Neumann, C. J., Grandel, H., Gaffield, W., Schulte-Merker, S. & Nüsslein-Volhard, C. Transient establishment of anteroposterior polarity in the zebrafish pectoral fin bud in the absence of sonic hedgehog activity. *Development* **126**, 4817–4826 (1999).
54. Fischer, S., Draper, B. W. & Neumann, C. J. The zebrafish *fgf24* mutant identifies an additional level of Fgf signaling involved in vertebrate forelimb initiation. *Development* **130**, 3515–3524 (2003).
55. Kucenas, S. *et al.* CNS-derived glia ensheath peripheral nerves and mediate motor root development. *Nat. Neurosci.* **11**, 143–151 (2008).
56. Smeeton, J., Askary, A. & Crump, J. G. Building and maintaining joints by exquisite local control of cell fate. *Wiley Interdiscip. Rev. Dev. Biol.* **6**, 1–22 (2017).
57. Kawakami, K., Asakawa, K., Muto, A. & Wada, H. *Tol2-mediated transgenesis, gene trapping, enhancer trapping, and Gal4-UAS system. Methods in Cell Biology* vol. 135 (Elsevier Ltd, 2016).
58. Westerfield, M. *The zebrafish book: a guide for the laboratory use of zebrafish (Danio rerio)*. (2000).
59. Saito, D. & Takase, Y. The Dorsal Aorta Initiates a Molecular Cascade That Instructs Sympatho-Adrenal Specification. *Science (80-)*. **336**, 1578–1581 (2012).
60. Jackman, W. R., Draper, B. W. & Stock, D. W. Fgf signaling is required for zebrafish tooth development. *Dev. Biol.* **274**, 139–157 (2004).

Figures

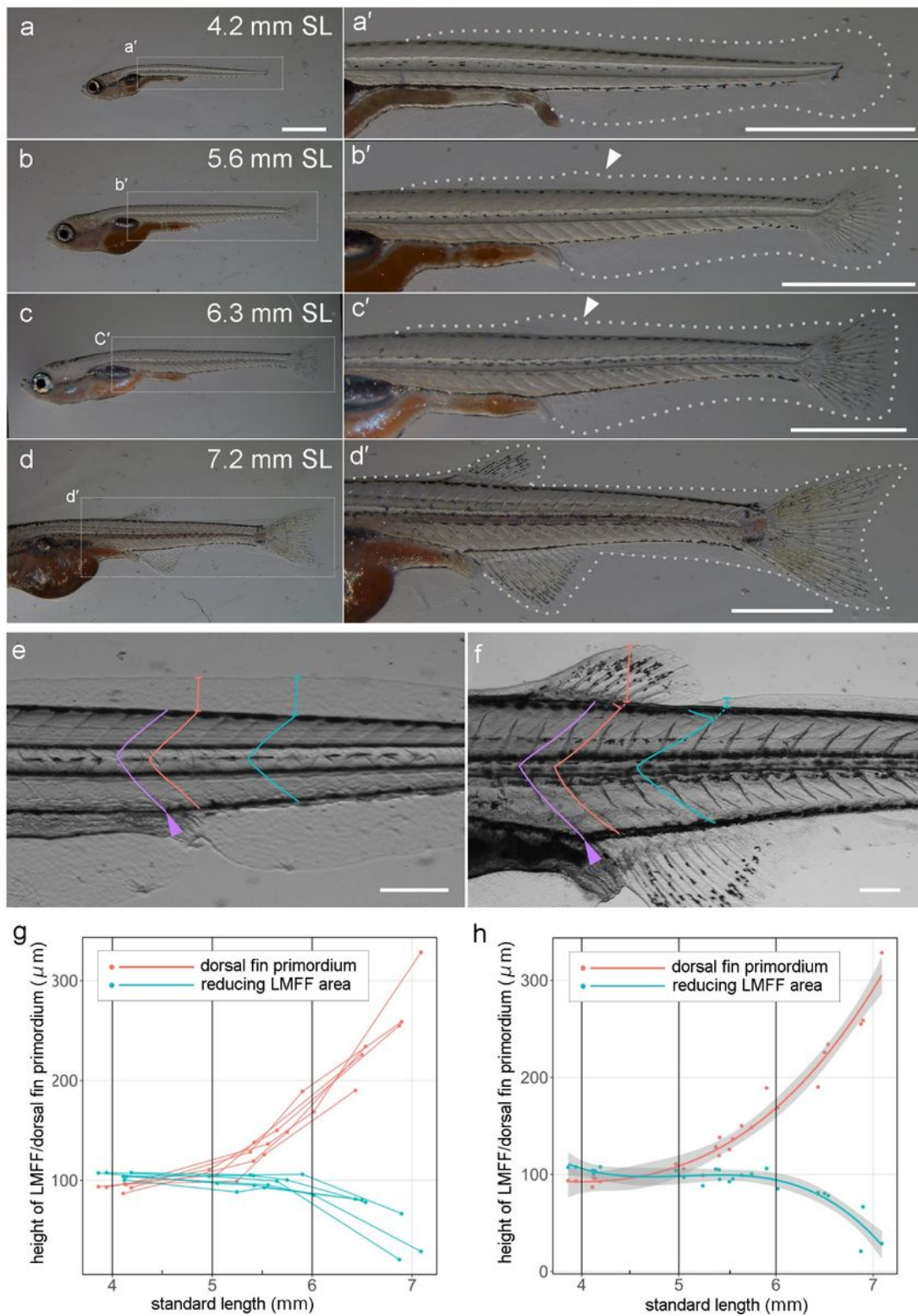


Figure 1

Morphological observation of dorsal fin development and LMFF reduction. (a-e) Gross anatomy of median fin development at 4.2 mm (a,a'), 5.6 mm (b,b'), 6.3 mm (c,c'), and 7.2 mm (d,d'). The right panels (a',b',c',d') are magnified views of the dashed rectangles in the left panes (a,b,c,d), respectively. White dashed lines in (a',b',c',d') indicate outlines of the LMFF. White arrowheads in (b',c') indicate protrusion sites of the LMFF. (e,f) Landmark and positions used for measuring the height of the LMFF. To examine

the height of the LMFF/dorsal fin primordium at the same position during ontogeny, we used the somite boundary, which is located at the gut tube bending point (purple arrowhead) as a landmark (the first boundary: purple line). Then, we measured two somite boundaries: the next somite boundary from the first boundary (red line) for the future dorsal fin position and the fourth somite boundary (blue lines) for the fin-disappearing positions, respectively. **(g,h)** Transition of height of the LMFF/dorsal fin primordium ($n = 6$). Each line in **(g)** indicates temporal transition of the same individual. **(h)** Local polynomial regression fit of **(g)**. The 95% confidence intervals are indicated as grey areas in **(h)**. Scale bars in **(a)** and those in **(a',b',c',d',e,f)** indicate 1 mm and 200 μm , respectively.

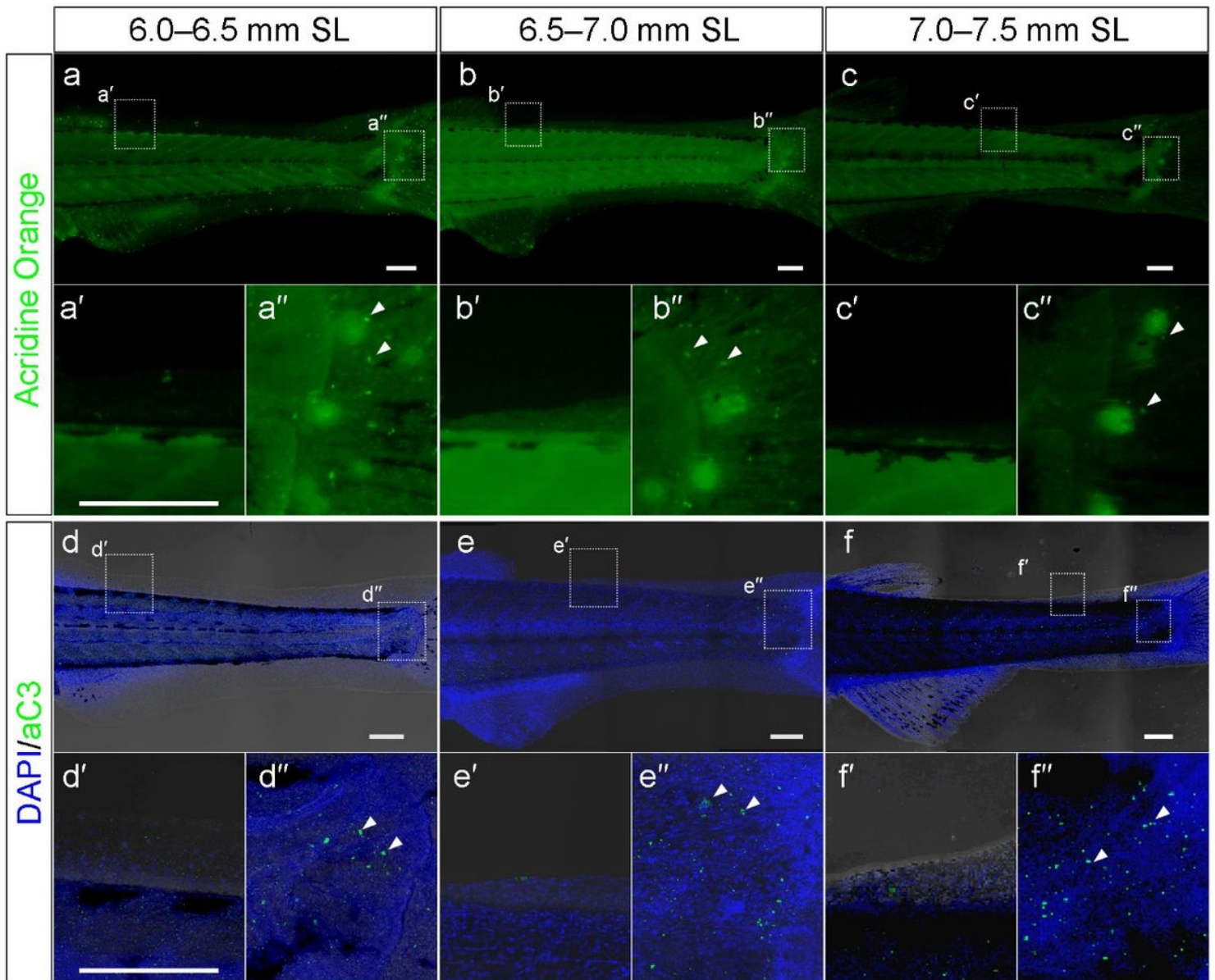


Figure 2

Apoptotic cell death in the reducing LMFF area. **(a-c'')** Acridine orange staining in the reducing LMFF area **(a',b',c')** and proximal part of the developing caudal fin region **(a'',b'',c'')** at 6.0–6.5 mm SL **(a-a'')**, 6.5–7.0 mm SL **(b-b'')**, and 7.0–7.5 mm SL **(c-c'')**. The lower panels **(a',a'',b',b'',c',c'')** are magnified views of the

dashed rectangles in the upper panels (a,b,c), respectively. (d-f'') Expression pattern of active caspase 3 in the reducing LMFF area (d',e',f') and proximal part of the developing caudal fin region (d'',e'',f'') area at 6.0–6.5 mm SL (d-d''), 6.5–7.0 mm SL (e-e''), and 7.0–7.5 mm SL (f-f''). The lower panels (d',d'',e',e'',f',f'') are magnified views of the dashed rectangles in the upper panels (d,e,f), respectively. Arrowheads in (a'',b'',c'',d'',e'',f'') indicate examples of apoptotic cell death signals. Scale bars indicate 200 μ m.

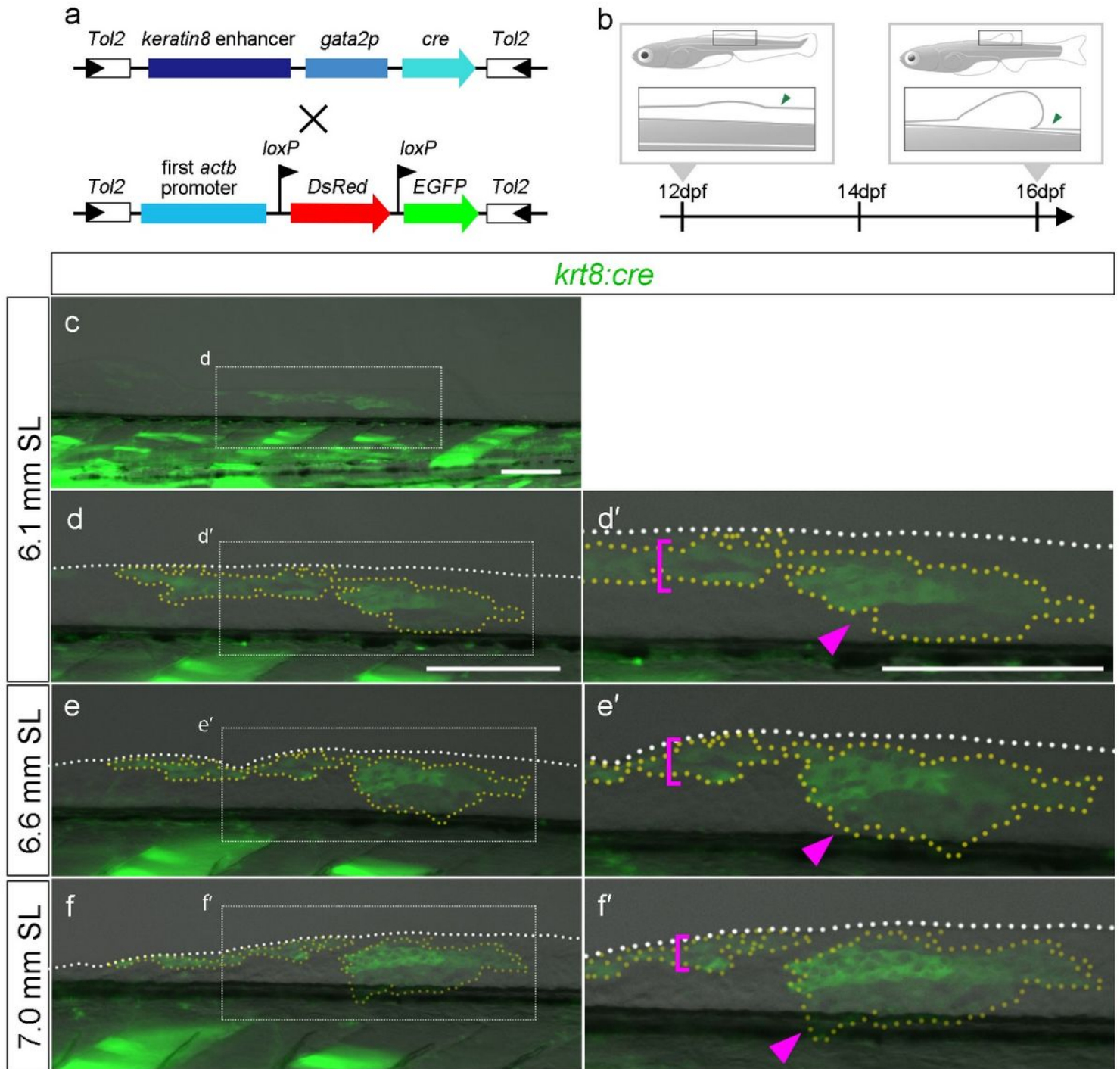


Figure 3

Cell-tracking analysis of the epithelial cells in the reducing LMFF area. (a) Schematic of the plasmid DNA construct used to generate the Tg. (b) Scheme of the Tg observation. (c-f') GFP-positive labelled cells in

the reducing LMFF area at 6.1 mm SL (**c-d'**), 6.6 mm SL (**e-e'**), and 7.0 mm SL (**f-f'**). The right panels (**d',e',f'**) are magnified views of the dashed rectangles in the left panes (**d,e,f**), respectively. White dashed lines in (**d',e',f'**) indicate outlines of the LMFFs. Yellow dashed lines indicate outlines of the EGFP-positive populations of epidermal cells. Magenta brackets in (**d',e',f'**) indicate EGFP-positive populations of epidermal cells experiencing proximo-distal shrinking. Magenta arrowheads in (**d',e',f'**) indicate EGFP-positive populations of epidermal cells migrating down to the trunk. Scale bars indicate 200 μ m.

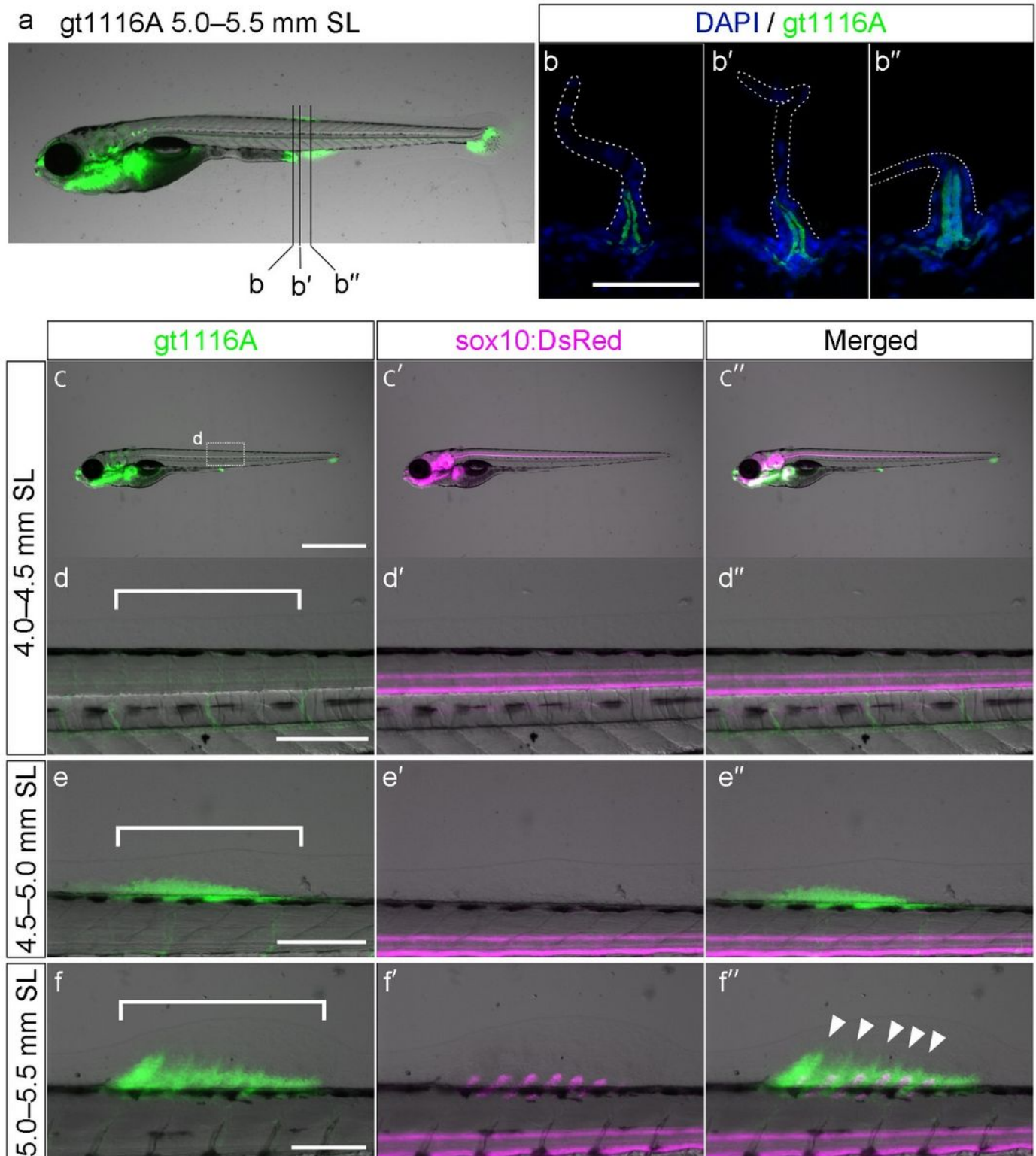


Figure 4

Expression pattern of UAS:EGFP in the *gt1116A* line and *sox10:DsRed* in the LMFF of double-transgenic zebrafish. **(a-b^{''})** Expression pattern of UAS:EGFP of the *gt1116A* line in the LMFF at 5.0–5.5 mm SL. Black lines in **(a)** indicate levels of the section shown in **(b-b^{''})**. White dashed lines in **(b-b^{''})** indicate outlines of the LMFFs. **(c-f^{''})** Expression pattern of UAS:EGFP of the *gt1116A* line and *sox10:DsRed* in the LMFF of double-transgenic fish at 4.0–4.5 mm SL **(c-d^{''})**, at 4.5–5.0 mm SL **(e-e^{''})**, and 5.0–5.5 mm SL **(f-f^{''})**. White brackets in **(d,e,f)** indicate future sites of the dorsal fins. White arrowheads in **(f^{''})** indicate distal expansion of the EGFP-positive mesenchymal cell population. Scale bars in **(b)** and those in **(c,d,e,f)** indicate 50 μ m and 200 μ m, respectively.

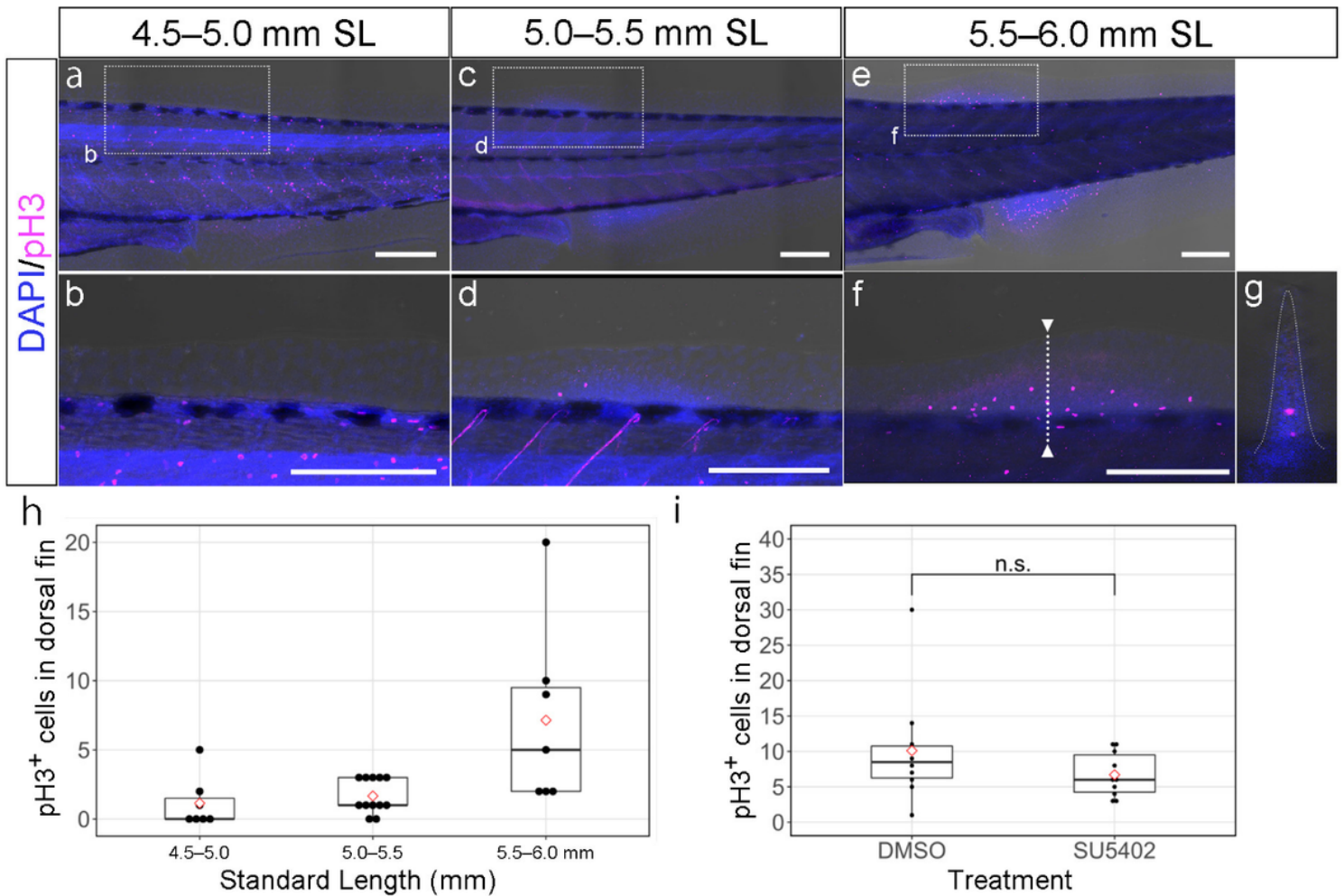


Figure 5

The expression pattern of phospho-histone-H3 in dorsal fin primordium. **(a-g)** Expression pattern of phospho-histone-H3 in the reducing LMFF area at 4.5–5.0 mm SL **(a,b)**, 5.0–5.5 mm SL **(c,d)**, and 5.5–6.0 mm SL **(e-g)**. The lower panels **(b,d,f)** are magnified views of the dashed rectangles in the upper panels **(a,c,e)**, respectively. **(g)** Optical sections of the dorsal fin primordium of the dashed line in **(f)**. The white dashed line in **(g)** indicates the outline of the LMFF. **(h)** Boxplots of phospho-histone-H3-positive cells in dorsal fin development along with the growth of the body. **(i)** Boxplots of phospho-histone-H3-

positive cells in dorsal fin development under SU5402 treatment. The proportions in **(h)** and **(i)** were calculated from the number of pH3-positive cells in dorsal fin primordium. Whiskers in **(h)** and **(i)** show maximum and minimum values within 1.5 times the interquartile range. Boxes show the median and 25th and 75th percentiles. The *P* value in **(i)** is the result of Welch's *t* test ($P = 0.2272$). Scale bars indicate 200 μm .

Supplementary Files

This is a list of supplementary files associated with this preprint. Click to download.

- [2022MiyamotoSupply0103.docx](#)